Age-Related Downregulation of CCN2 Is Regulated by Cell Size in a YAP/TAZ-Dependent Manner in Human Dermal Fibroblasts: Impact on Dermal Aging

Zhaoping Qin[1], Tianyuan He[1], Chunfang Guo[1] and Taihao Quan[1]

CCN2, a member of the CCN family of matricellular proteins, is a key mediator and biomarker of tissue fibrosis. We previously reported that CCN2 is significantly reduced in aged human dermis, which contributes to dermal aging through the downregulation of collagen production, the major structural protein in the skin. In this study, we investigated the underlying mechanisms of the age-related downregulation of CCN2 in human skin dermal fibroblasts. Dermal fibroblasts isolation and laser-capture microdissection–coupled RT-PCR from human skin confirmed that age-related reduction of CCN2 expression is regulated by epigenetics. Mechanistic investigation revealed that age-related reduction of CCN2 is regulated by impaired dermal fibroblast spreading/cell size, which is a prominent feature of aged dermal fibroblasts in vivo. Gain-of-function and loss-of-function analysis confirmed that age-related downregulation of CCN2 is regulated by YAP/TAZ in response to reduced cell size. We further confirmed that restoration of dermal fibroblast size rapidly reversed the downregulation of CCN2 in a YAP/TAZ-dependent manner. Finally, we confirmed that reduced YAP/TAZ nuclear staining is accompanied by loss of CCN2 in aged human skin in vivo. Our data reveal a mechanism by which age-related reduction in fibroblast spreading/size drives YAP/TAZ-dependent downregulation of CCN2 expression, which in turn contributes to loss of collagen in aged human skin.

JID Innovations (2022);**2:**100111 doi:10.1016/j.xjidi.2022.100111

INTRODUCTION

Collagen is the major structural protein in the skin and is primarily produced by dermal fibroblasts. Loss of collagen is a prominent feature of aged human skin that significantly contributes to dermal aging (Quan and Fisher, 2015; Uitto, 1986). Age-related loss of collagen impairs the structural and mechanical integrity of the skin, which creates a tissue microenvironment conducive to skin disorders such as increased fragility (Lavker, 1979; Uitto and Bernstein, 1998), impaired vasculature support (Ashcroft et al., 1995; Jacob, 2003), delayed wound healing (Ashcroft et al., 2002; Eaglstein, 1989; Thomas, 2001), and cancer development (Bissell and Hines, 2011; Bissell et al., 2005; Ingber, 2008; Pickup et al., 2014).

In young healthy skin, dermal fibroblasts interact with intact collagen fibrils, through collagen-binding integrins, to achieve and maintain a stretched morphology (Fisher et al., 2008; Varani et al., 2004). However, collagen fibrils in aged skin become fragmented and disorganized, which impairs collagen–fibroblast interactions and results in reduced spreading and cell size (Fisher et al., 2008; Qin et al., 2014b; Varani et al., 2004). We previously reported that age-related reductions in dermal fibroblast size are a prominent feature of aged human skin in vivo and have a significant impact on dermal aging (Fisher et al., 2009, 2008; Qin et al., 2014b). Reduction of dermal fibroblast size not only impairs dermal fibroblast collagen production (Fisher et al., 2016; Quan et al., 2013b) but also promotes collagen fragmentation through the upregulation of multiple matrix metalloproteinases (Fisher et al., 2009; Qin et al., 2017, 2014b; Quan et al., 2013a).

CCN2, also known as CTGF, is a second member of the CCN family of proteins (Perbal, 2004; Twigg, 2018). CCN2 is a secreted, cysteine-rich matricellular protein that exhibits diverse biological activities in vitro such as cell proliferation, adhesion, migration, and extracellular matrix (ECM) production (McLennan et al., 2013; Moussad and Brigstock, 2000). CCN2 stimulates collagen and ECM synthesis when injected into mouse skin or added to cultured fibroblasts (Duncan et al., 1999). *Ccn2*-null mice die shortly after birth owing primarily to respiratory failure caused by skeletal defects (Ivkovic et al., 2003), indicating that CCN2 plays a crucial role in the regulation of cartilage ECM production during development. Several lines of evidence indicate that CCN2 is markedly elevated in numerous fibrotic disorders involving the skin, lungs, and kidneys, where it is believed to stimulate excessive collagen deposition (Kubota and

[1]*Department of Dermatology, University of Michigan Medical School, Ann Arbor, Michigan, USA*

Correspondence: Taihao Quan, Department of Dermatology, University of Michigan Medical School, 1301 Catherine, Medical Science I, Room 6447, Ann Arbor, Michigan 48109-0609, USA. E-mail: thquan@umich.edu

Abbreviations: 3D, three-dimensional; AFM, atomic force microscopy; ECM, extracellular matrix; Lat-A, latrunculin-A; LCM, laser-capture microdissection; PPD, population doubling; siRNA, small interfering RNA

Received 20 October 2021; revised 22 December 2021; accepted 28 December 2021; accepted manuscript published online XXX; corrected proof published online XXX

Cite this article as: JID Innovations 2022;2:100111

Takigawa, 2015). CCN2 appears to be primarily involved in the differentiation of fibroblast-derived progenitor cells into myofibroblasts (Kapoor et al., 2008; Liu et al., 2010). Therefore, targeting fibroblast-specific CCN2 is considered an antifibrotic therapeutic approach (Leask, 2020; Liu et al., 2013).

In contrast to fibrotic disease, CCN2 is significantly downregulated in aged human skin (Quan et al., 2010). Reduced expression of CCN2 contributes to dermal aging through the downregulation of collagenous ECM production (Quan et al., 2010). However, the underlying mechanism(s) responsible for the reduction of CCN2 expression observed in aged human skin is largely unknown. *CCN2* was first identified as a YAP-target gene by Leask et al. (2003). CCN2 has now emerged as a bona fide transcriptional target of YAP and TAZ (Urtasun et al., 2011; Zhao et al., 2010). YAP and TAZ are originally recognized as key effectors of the hippo signaling pathway, which play a pivotal role in controlling organ size and maintaining tissue homeostasis (Moya and Halder, 2019). Hippo signaling protein kinase complex LATS1/2 phosphorylates multiple serine residues of YAP and TAZ. On phosphorylation, YAP and TAZ are sequestered in the cytoplasm by interaction with 14-3-3 proteins, followed by ubiquitination and proteasomal degradation. Interestingly, YAP/TAZ function is predominantly regulated by cell size and mechanical tension independent of the hippo pathway (Dupont et al., 2011; Panciera et al., 2017). Increases in cell spreading/mechanical force cause YAP and TAZ to localize in the nucleus where they regulate target gene transcription. Conversely, reduced cell spreading/mechanical force causes YAP/TAZ to be sequestered in the cytosol, thereby preventing their transcriptional activity.

Although *CCN2* has been recognized as a YAP/TAZ-target gene, CCN2 often represents a simple readout of YAP/TAZ activity rather than a functional effector of YAP/TAZ signaling. Furthermore, the role of CCN2 in mediating YAP/TAZ function in human skin is virtually unknown. In this study, we report that the downregulation of CCN2 in aged human skin is induced, in a YAP/TAZ-dependent manner, by reductions in dermal fibroblast size. These data reveal a mechanism by which changes in dermal fibroblast size regulate both YAP/TAZ nuclear translocation and CCN2 expression.

RESULTS

Age-related reduction of CCN2 expression is regulated by epigenetics

Primary dermal fibroblasts were utilized to investigate the potential mechanisms by which CCN2 is reduced with age (Quan et al., 2013b, 2010). CCN2 is predominantly expressed in primary human dermal fibroblasts compared with that in primary epidermal keratinocytes (Figure 1a). Therefore, we assessed CCN2 expression by isolating dermal fibroblasts from young (mean age of 27±1 years, n = 6) and aged (mean age of 83±1.4 years, n = 6) human buttock skin and culturing them without passage (Figure 1b). Interestingly, we found that the expression of *CCN2* mRNA and protein was similar between the fibroblasts isolated from young skin and those from aged skin (Figure 1b). However, laser-capture microdissection (LCM)–coupled RT-PCR indicated that *CCN2* mRNA expression was significantly reduced in aged dermal fibroblasts compared with that in young dermal fibroblasts in vivo (Figure 1c). Consistent with this observation, dermal CCN2 protein expression was significantly reduced in aged dermis compared with that in young dermis (Figure 1d). These data indicate that age-related reductions in CCN2 expression are likely due to epigenetic changes rather than intrinsic genetic alteration. Furthermore, at early (population doubling [PPD]4) and late (PPD20) population doublings, *CCN2* mRNA expression was comparable (Figure 1e), suggesting that in vitro cellular aging does not influence *CCN2* mRNA expression.

We previously reported that a significant feature of aged dermal fibroblasts is decreased cell size accompanied by reduced spreading and a collapsed shape (Fisher et al., 2009; Qin et al., 2017, 2014b; Quan et al., 2013b). Functionally, reduced dermal fibroblast size inhibits collagen production and thus contributes to human dermal aging. These human skin in vivo observations led us to continue exploring the connection between reduced dermal fibroblast size and CCN2 expression.

Reduced dermal fibroblast size downregulates CCN2 expression

Dermal fibroblast size was manipulated with latrunculin-A (Lat-A) treatment, which rapidly blocks actin polymerization and reduces cell size (Gieni and Hendzel, 2008). As expected, cells decreased in size once actin polymerization was blocked (Figure 2a, right panel). Staining of the actin cytoskeleton with phalloidin indicated a loss of actin cytoskeletal fibers and a reduction in cell surface area by approximately 75% (Figure 2a, panel). Importantly, a decrease in fibroblast size markedly reduced the levels of *CCN2* mRNA (Figure 2b) and protein (Figure 2c and d) by approximately 70%.

Dermal fibroblasts normally reside in a collagen-rich, three-dimensional (3D) ECM microenvironment in human skin. Accordingly, we used a 3D collagen gel model to investigate the effects of fibroblast size on CCN2 expression. Cell size in the 3D collagen gel was reduced by treatment with recombinant human matrix metalloproteinase 1, which fragments collagen fibrils and thereby interrupts cell–collagen interactions. Consistent with a monolayer culture, cell size in the 3D collagen gel (Figure 2e) was reduced, and significant downregulation of *CCN2* mRNA expression was observed (Figure 2f). To confirm these observations, cells were cultured on poly-L-lysine–coated surfaces (Figure 2g), which allow for integrin-independent attachment, thus limiting cell spreading and cell size (Mazia et al., 1975). As a result, *CCN2* mRNA expression was significantly reduced (Figure 2h). Together, these data show that decreases in fibroblast size limit CCN2 expression, suggesting a possibility that downregulation of CCN2 in aged human skin is regulated by cell size.

Reductions in dermal fibroblast size impede YAP/TAZ nuclear translocation, causing CCN2 downregulation

We investigated the potential mechanisms by which CCN2 expression is decreased in response to reduced cell size. CCN2 expression is controlled by YAP/TAZ, whose activity is regulated by subcellular localization in response to changes

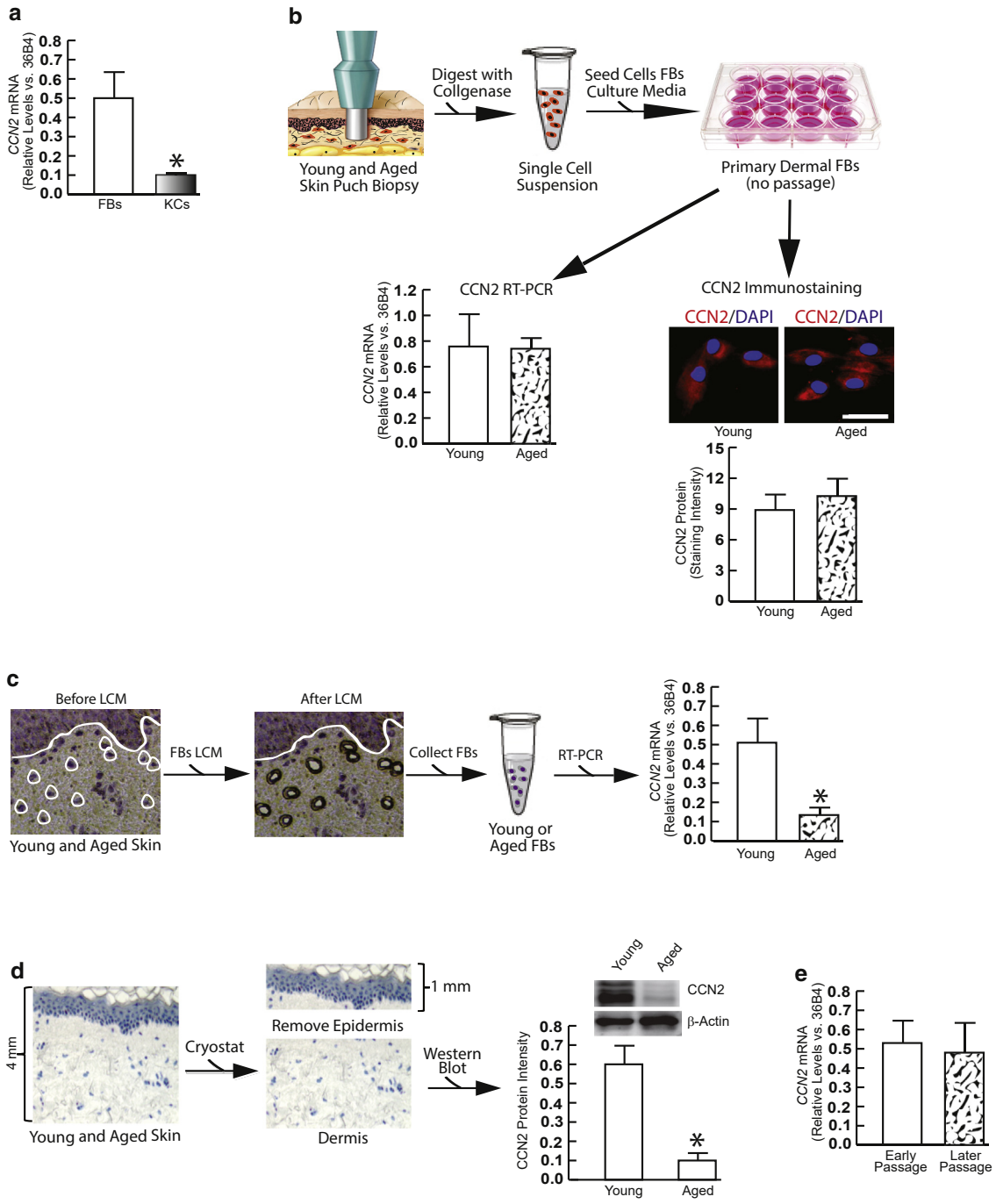

Figure 1. Age-related reduction of CCN2 expression is regulated by epigenetics. (**a**) Skin fibroblasts and keratinocytes were prepared from punch biopsies obtained from young (mean age of 27 ± 1 years, n = 6) and aged (mean age of 83 ± 1.4 years, n = 6) buttock skin (see Materials and Methods for details). Total RNA was prepared and *CCN2* mRNA levels were quantified by real-time RT-PCR and normalized to the housekeeping gene *36B4*. Data represent cells from six young and six aged subjects. Mean ± SEM. **P* < 0.05. (**b**) Fibroblasts isolated from young and aged skin similarly express *CCN2* mRNA and protein. Dermal fibroblasts were prepared from punch biopsies obtained from young (mean age of 27 ± 1 years, n = 6) and aged (mean age of 83 ± 1.4 years, n = 6) buttock skin (see Materials and Methods for details). *CCN2* mRNA levels were quantified by real-time RT-PCR and normalized to the housekeeping gene *36B4* (lower left). CCN2 protein levels were determined by immunostaining and quantified by ImageJ (National Institutes of Health, Bethesda, MD) (lower right). CCN2 protein levels were expressed in staining intensity after normalization by cell count. Nuclei were stained with DAPI (blue). Data represent cells from six young and six aged subjects. Bar = 50 µm. Mean ± SEM. (**c**) Skin punch biopsies obtained from young (mean age of 27 ± 1 years, n = 6) and aged (mean age of 83 ± 1.4 years, n = 6). Dermal fibroblasts were captured by laser-capture microdissection, and *CCN2* mRNA levels were determined by real-time RT-PCR. Data represent cells from six young and six aged subjects. Mean ± SEM. **P* < 0.05. (**d**) Skin punch biopsies (4 mm) obtained from young (mean age of 27 ± 1 years, n = 6) and aged (mean age of 83 ± 1.4 years, n = 6). The epidermis was removed by cryostat to cut to a depth of 1 mm, after which dermal CCN2 protein expression was determined by western blot and normalized by β-actin (loading control) for quantification. The Inset shows representative images. Data represent dermal tissues from six young and six aged subjects. Mean ± SEM. **P* < 0.05. (**e**) *CCN2* mRNA expression is not altered by in vitro cellular aging. Total RNA was extracted from the fibroblasts at early (PPD4) and late (PPD20) population doublings. *CCN2* mRNA levels were quantified by real-time RT-PCR and normalized to the housekeeping gene *36B4*. Data represent cells from six PPD4 and six PPD20. Mean ± SEM. **P* < 0.05. FB, fibroblast; KC, keratinocyte; LCM, laser-capture microdissection; PPD, population doubling.

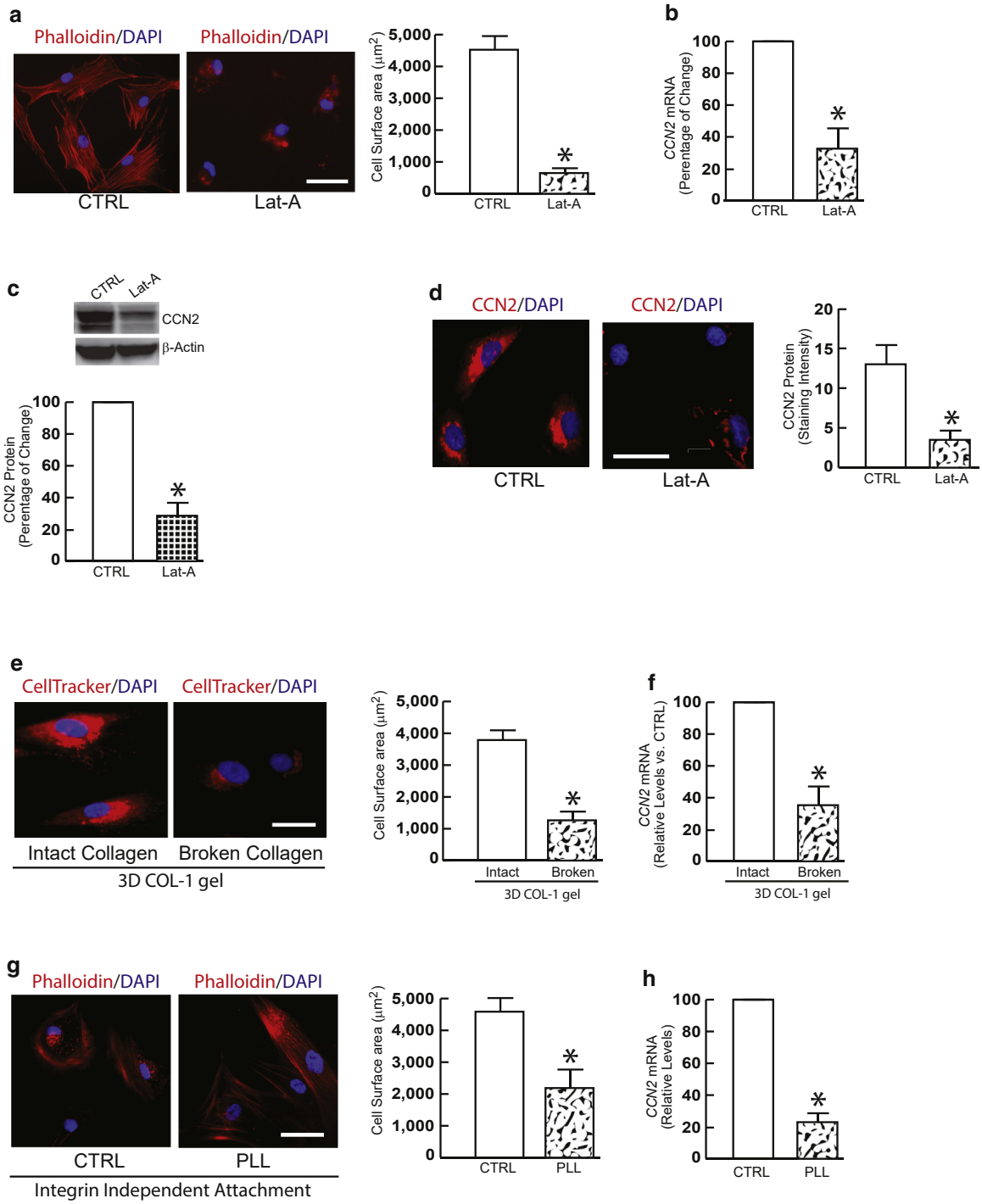

Figure 2. Reduced dermal fibroblast size downregulates CCN2 expression. (**a**) Reduced fibroblast size by actin cytoskeleton disruption. Cells were stained with phalloidin (red) and DAPI (blue), and relative cell surface areas were quantified by ImageJ. Data are representative of three independent experiments. Mean ± SEM. *$P < 0.05$. Bar = 50 μm. (**b**) *CCN2* mRNA expression, measured by real-time RT-PCR, is downregulated by reduced fibroblast size. Data are representative of six independent experiments. Mean ± SEM. *$P < 0.05$. (**c**) CCN2 protein expression is downregulated by reduced fibroblast size. The inset shows representative images. Data are representative of four independent experiments. Mean ± SEM. *$P < 0.05$. (**d**) CCN2 protein expression is downregulated by reduced fibroblast size. CCN2 protein levels were determined by immunostaining and quantified by ImageJ. CCN2 protein levels were expressed in staining intensity after normalization by cell count. Nuclei were stained with DAPI (blue). Data are representative of four independent experiments. Mean ± SEM. *$P < 0.05$. Bar = 50 μm. (**e**) Reduced fibroblast size induced by rhMMP-1 in 3D collagen gels. Collagen gels were stained with CellTracker (red) and DAPI (blue). Relative cell surface areas were quantified by ImageJ. Data are representative of four independent experiments. Mean ± SEM. *$P < 0.05$. Bars = 50 μm. (**f**) *CCN2* mRNA expression is also downregulated by rhMMP-1–treated collagen gels, which lead to reduced fibroblast size. *CCN2* mRNA levels were quantified by real-time RT-PCR and normalized to the housekeeping gene *36B4*. Data are representative of four independent experiments. Mean ± SEM. *$P < 0.05$. (**g**) Reduced fibroblast size by limitation of cell spreading. Cells were plated on a regular tissue culture plate (left) or PLL-coated plate (right) for 24 hours and stained with phalloidin (red). Nuclei were stained with DAPI (blue). Cell surface area was quantified by ImageJ. Mean ± SEM. *$P < 0.05$. Data are representative of three independent experiments. Bar = 50 μm. (**h**) *CCN2* mRNA expression is downregulated by reduced fibroblast size. Total RNA was prepared from a regular

in cell size (Dupont et al., 2011; Zhao et al., 2011). We confirmed that YAP/TAZ was localized to the nuclei of control fibroblasts and that reduced cell size by Lat-A treatment inhibited its nuclear translocation (Figure 3a). Next, we assessed whether changes in CCN2 expression were mediated by cytosolic YAP/TAZ in fibroblasts with reduced size by Lat-A treatment. To test this, YAP/TAZ nuclear translocation was restored by introducing YAP/TAZ-mutant plasmids (see Materials and Methods for details), which promote constitutive YAP/TAZ nuclear translocation (Chan et al., 2011). As expected, reductions in cell size by Lat-A treatment significantly decreased CCN2 expression, whereas CCN2 remained unaltered by an introduction of YAP/TAZ-mutant plasmids (Figure 3b). We confirmed the data mentioned earlier by manipulating cell size: culturing cells in 3D-broken collagen gel (Figure 3c) and poly-L-lysine–coated surfaces (Figure 3d), as shown in Figure 2e and g. In both conditions, reductions in cell size significantly decreased CCN2 expression and that restored by the introduction of YAP/TAZ-mutant plasmids. These data confirmed that CCN2 is regulated by cell size in a YAP/TAZ-dependent manner, as observed in Lat-A–treated cells (Figure 3b). Together, these data indicate that downregulation of CCN2, in fibroblasts with reduced size, is mediated by the inability of YAP/TAZ to translocate to the nucleus.

Restoring dermal fibroblast size re-establishes YAP/TAZ nuclear translocation and CCN2 expression

We assessed whether the downregulation of CCN2 expression could be reversed by restoring fibroblast size. For these studies, Lat-A–containing media were added for 24 hours and replaced with fresh culture media after washing. With the removal of Lat-A, fibroblasts transformed from a small, rounded morphology to a typical elongated morphology (Figure 4a). After withdrawal of Lat-A–containing media, cell surface area was restored (Figure 4a, chart). Consistent with the restored morphology of dermal fibroblasts, YAP/TAZ nuclear translocation was re-established (Figure 4b), and CCN2 expression returned to the basal levels (Figure 4c).

Cell size–dependent reversibility of CCN2 and type I collagen expression is mediated by YAP/TAZ

Next, we assessed whether cell size–dependent reversibility of CCN2 and type I collagen expression were mediated by YAP/TAZ. To investigate this, we first confirmed *YAP/TAZ* knockdown levels by YAP/TAZ small interfering RNAs (siRNAs) (Figure 5a). Knockdown of *YAP/TAZ* resulted in the reduction of CCN2 and type I collagen expression (Figure 5b), suggesting that CCN2 and type I collagen are regulated by YAP/TAZ. Cell morphology was restored within 2 hours of Lat-A removal in the fibroblasts transfected with control siRNA (Figure 5c, left panels, phalloidin) and *YAP/TAZ* siRNA (Figure 5d, left panels, phalloidin). Consistently, YAP/TAZ nuclear translocation (Figure 5c, middle panel) and CCN2 expression (Figure 5c, right panel) recovered within 2 hours of Lat-A removal in the fibroblasts transfected with control siRNA (Figure 5c). Importantly, reversibility of CCN2 downregulation was not observed on Lat-A removal when *YAP/TAZ* was knocked down (Figure 5d, right panels). *CCN2* mRNA expression confirmed this observation (Figure 5e). As expected, cell size–dependent reductions in type I collagen were reversed when Lat-A was removed (Figure 5g, left, control-targeting siRNA). However, in the same conditions with *YAP/TAZ* knockdown, the reversal of type I collagen was absent in both mRNA (Figure 5f, right, *YAP/TAZ*-targeting siRNA) and protein (Figure 5g, right, *YAP/TAZ*-targeting siRNA). Next, we manipulated cells size by culturing cells in either mechanically constrained or unconstrained 3D collagen matrices (Figure 5h). The mechanical constraint was achieved by incorporating a nylon mesh disk within the matrices (Fisher et al., 2016). The rigidity of the disk counteracted the traction force of the fibroblasts and thereby prevented contraction of the matrices (Figure 5h, top middle and right panels). Fibroblasts in restrained matrices displayed elongated and spread morphology (Figure 5h, second top middle and right panels). In contrast, fibroblasts in unconstrained matrixes displayed a small and contracted appearance (Figure 5h, second top left panel). As expected, we confirmed that reductions in cell size (unconstrained gel) reduced CCN2 and type I collagen expression and impeded YAP/TAZ nuclear translocation (Figure 5h, left panels and bar graph). In contrast, elongated cells in restrained matrices displayed high levels of CCN2 and type I collagen expression and YAP/TAZ nuclear translocation (Figure 5h, middle panels and bar graph). Importantly, the high levels of CCN2 and type I collagen expression in elongated cells were significantly reduced when *YAP/TAZ* was knocked down (Figure 5h, right panels and bar graph). Together, these data indicate that YAP/TAZ regulates CCN2 and type I procollagen expression and that cell size–dependent reversibility of CCN2 and type I collagen expression is mediated by YAP/TAZ activity.

Downregulation of YAP/TAZ is accompanied by reduced CCN2 and type I collagen expression in aged human skin in vivo

We investigated YAP/TAZ expression after CCN2 and type I collagen downregulation in aged human dermis. Human skin biopsies were obtained from sun-protected buttock skin and stratified into young (aged 26.7 ± 1.3 years) and aged (aged 84.0 ± 1.7 years) groups. YAP/TAZ staining was significantly decreased with age and was accompanied by reduced expression of CCN2 and type I procollagen (Figure 6a and b). These data suggest that concomitant downregulation of YAP/TAZ and CCN2 in response to reduced fibroblast size may contribute to human dermal aging.

DISCUSSION

In this study, we show that reduced fibroblast size, a prominent feature of aged dermal fibroblasts, leads to the downregulation of CCN2 in aged human skin. On further examination, we discovered that cell size–dependent downregulation of CCN2 is mediated by YAP/TAZ, which is predominantly regulated by cell size and mechanical tension

tissue culture plate (CTRL) or PLL-coated plate. *CCN2* mRNA levels were quantified by real-time RT-PCR and normalized to the housekeeping gene *36B4*, as an internal control. Data are representative of four independent experiments. Mean ± SEM. N = 4. *$P < 0.05$. 3D, three-dimensional; COL-1, type 1 collagen; CTRL, control; Lat-A, Latrunculin-A; MMP-1, matrix metalloproteinase 1; PLL, poly-L-lysine; rhMMP-1, recombinant human matrix metalloproteinase 1.

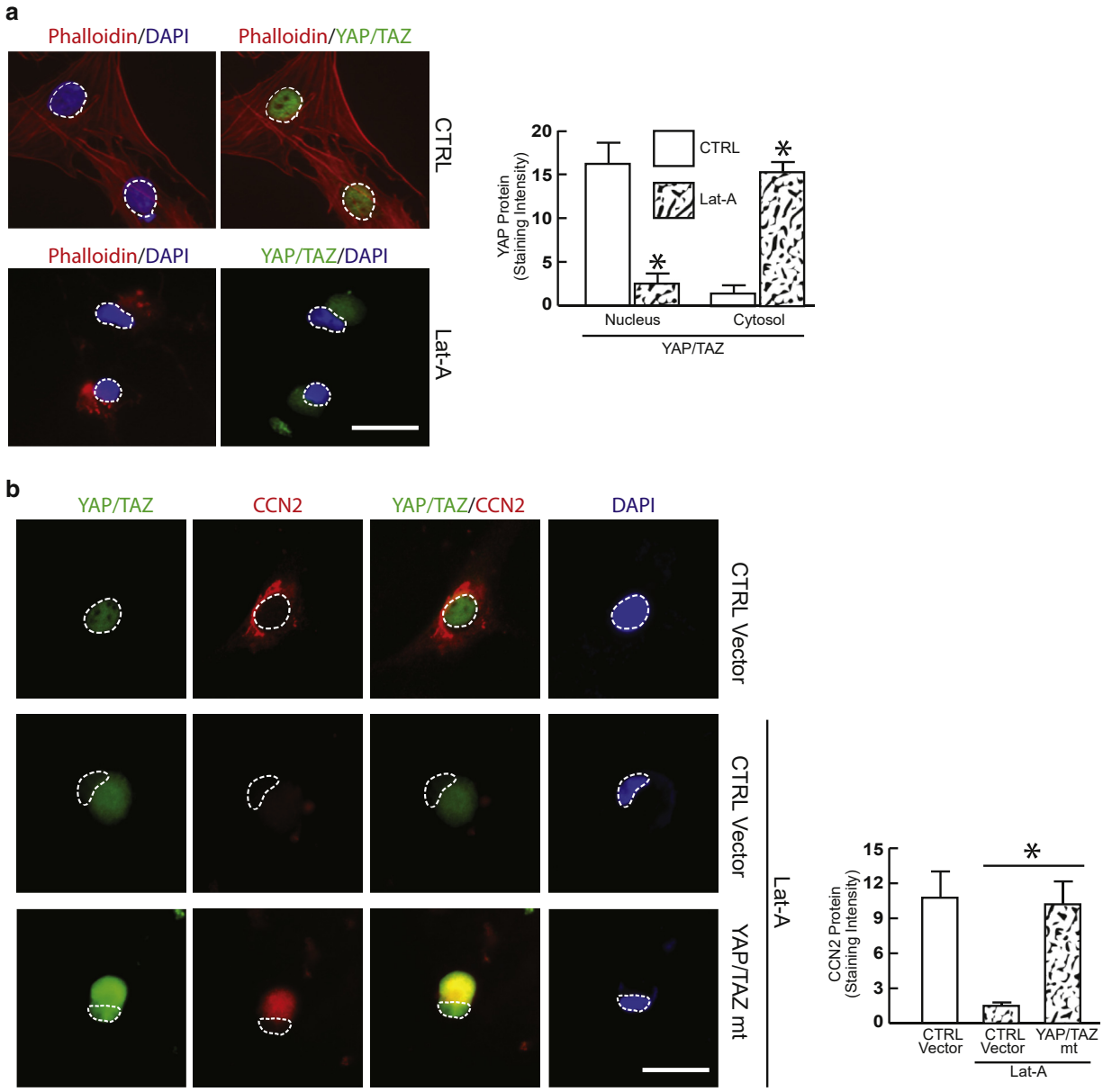

Figure 3. Downregulation of CCN2 by reduced dermal fibroblast size is mediated by impaired YAP/TAZ nuclear translocation. (**a**) YAP/TAZ nuclear translocation is impeded by reduced fibroblast size. Dermal fibroblasts were treated with DMSO (CTRL) or Lat-A (180 nM) for 24 hours. YAP and TAZ protein levels were determined by immunostaining and quantified by ImageJ (National Institutes of Health, Bethesda, MD). YAP and TAZ protein levels were expressed in staining intensity after normalization by cell count. Nuclei showed blue fluorescence (DAPI). Data are representative of three independent experiments. Mean ± SEM. $*P < 0.05$. Bar = 50 μm. (**b**) Downregulation of CCN2 by reduced dermal fibroblast size is reversed by YAP/TAZ nuclear translocation. Impeded YAP/TAZ nuclear translocation was restored by overexpression of YAP/TAZ-mutant plasmids, which allow for constitutive YAP/TAZ nuclear translocation. CCN2 protein levels were determined by immunostaining and quantified by ImageJ. CCN2 protein levels were expressed in staining intensity after normalization by cell count. Nuclei were stained with DAPI (blue). Data are representative of three independent experiments. Mean ± SEM. $*P < 0.05$. Bar = 50 μm. (**c, d**) Cells were transfected with control and YAP/TAZ-mutant plasmids for 48 hours. (**c**) Transfected cells were embedded in intact collagen gel and rhMMP-1–treated partially broken collagen gel. (**d**) Transfected cells were plated on regular tissue culture plate (CTRL) or PLL-coated plate. CCN2, YAP, and TAZ protein levels were determined by capillary electrophoresis immunoassay. CCN2 and β-actin levels were determined from cytoplasmic protein fractions, and YAP/TAZ levels were determined from nuclear protein fractions. The chemiluminescence signal of the specific protein from the capillary tube was obtained directly from the capillary system (Compass software, ProteinSimple, Santa Clara, CA), and the data were displayed by lane in a virtual-blot image, which was simulated using the signal intensity (chemiluminescence) of the specific protein. The tables show the quantitative results from the chemiluminescence signals detected by the specific protein from the capillary tubes. The chemiluminescence signal of the CCN2 protein was normalized to β-actin (loading control), and the data were expressed as a percent of control (bar charts). Data are representative of four independent experiments. Mean ± SEM. $*P < 0.05$. 3D, three-dimensional; COL-1, type 1 collagen; CTRL, control; Lat-A, Latrunculin-A; mt, mutant; PLL, poly-L-lysine; rhMMP-1, recombinant human matrix metalloproteinase 1.

(Dupont et al., 2011; Panciera et al., 2017). *CCN2* is well-recognized as a prominent YAP/TAZ-target gene; however, its role in mediating YAP/TAZ function is poorly understood. Our study proposes a mechanism by which age-related reductions in fibroblast size drive YAP/TAZ-dependent downregulation of CCN2 expression, which in turn contributes to loss of collagen (Figure 6c). Our data also propose a positive feedback loop in which age-related reductions in

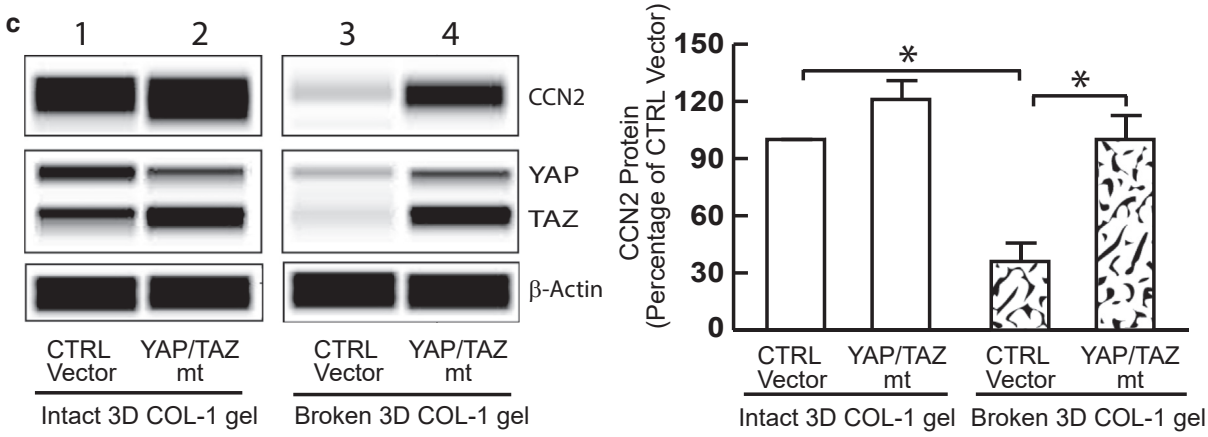

Signal Intensity (chemiluminescence)				
Proteins	1	2	3	4
CCN2	17,012	18,150	2,780	15,843
YAP	7,432	6,982	2,036	5,968
TAZ	5,069	7,259	1,856	7,015
β-Actin	17,096	16,245	16,514	17,689

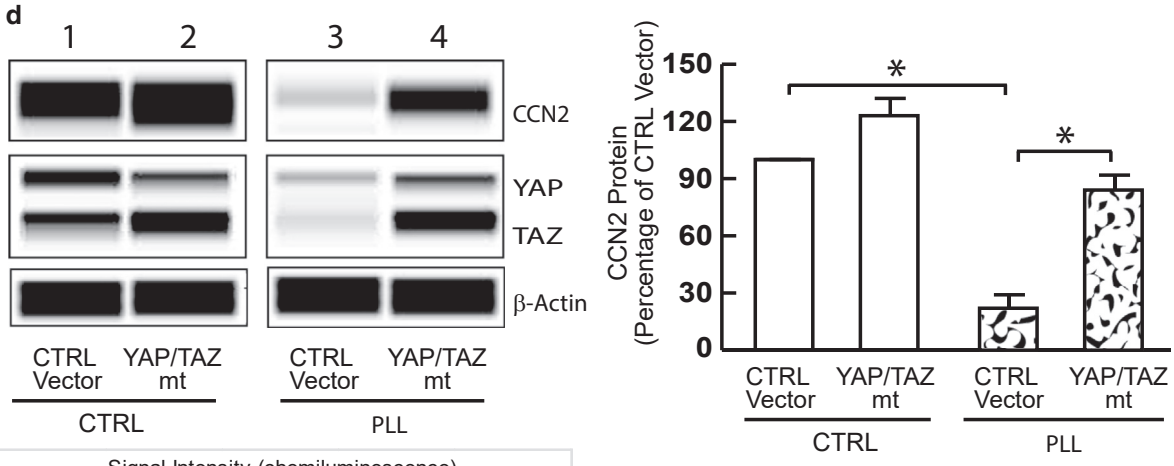

Signal Intensity (chemiluminescence)				
Proteins	1	2	3	4
CCN2	16,259	18,524	2,998	15,052
YAP	6,826	5,847	2,105	5,014
TAZ	4,251	5,826	1,705	5,926
β-Actin	16,952	15,987	14,892	15,047

Figure 3. Continued.

fibroblast size increasingly contribute to collagen deficiency in aged human skin (Figure 6c). We propose a model in which collagen deficiency, by interrupting cell–collagen interactions, leads to a reduction in fibroblast size and YAP/TAZ activity, thereby decreasing the production of CCN2 and collagen. This feedback loop extends our current understanding of human dermal aging by identifying age-related and fibroblast size–dependent downregulation of YAP/TAZ and CCN2 as critical factors promoting age-related dermal thinning.

Fibroblasts are the major collagen-producing cells in the dermis, and their spreading and size largely depend on interaction with surrounding collagen fibrils. In the young healthy dermis, fibroblasts interact with intact collagen fibrils to maintain basal spreading and size. However, in aged human dermis, fragmented collagen fibrils are unable to provide adequate binding for fibroblasts and mechanical resistance to traction forces generated from them (Fisher et al., 2008; Qin et al., 2014b; Varani et al., 2004). Therefore, the collagenous microenvironment in the aged dermis is unable to provide sufficient mechanical tension to maintain fibroblast spreading and size. Cell size influences multiple cellular functions, including signal transduction, gene expression, and metabolism (Geiger et al., 2009; Ingber, 2008). In addition to these known functions, we report that cell size can control the expression of CCN2 in fibroblasts. In agreement with this notion, we previously reported that enhancement of mechanical and structural support within the dermis by direct injection of dermal filler (cross-linked

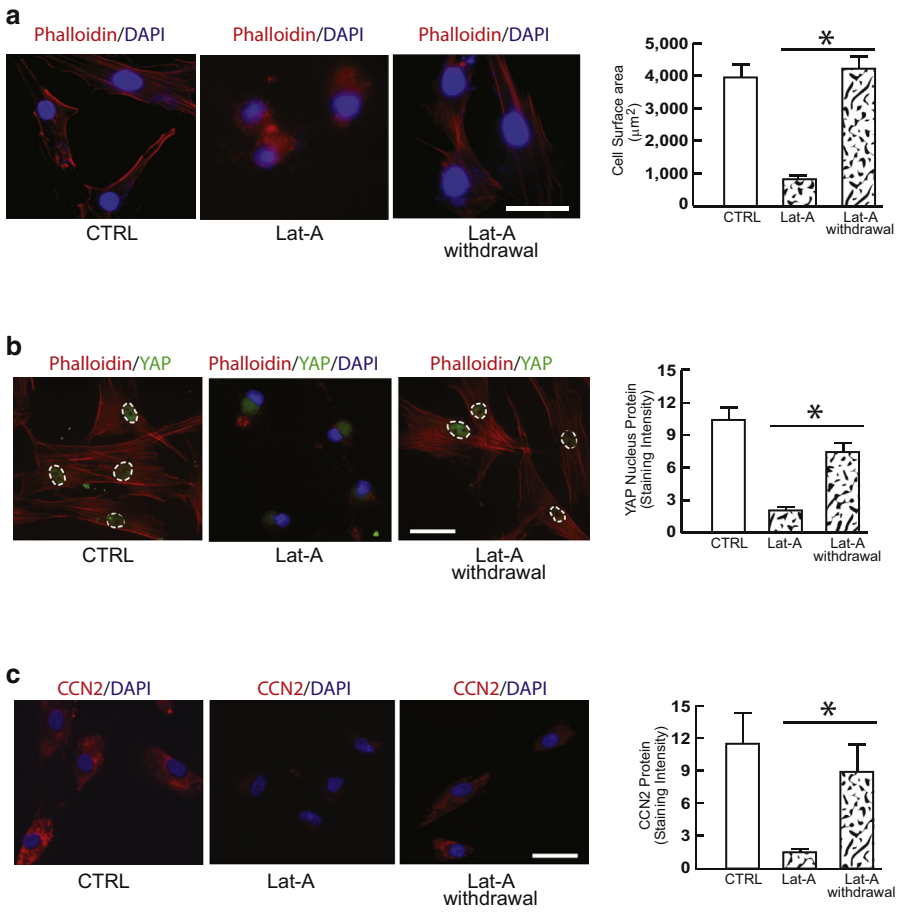

Figure 4. Restoration of dermal fibroblast size reversed the inhibition of YAP/TAZ nuclear translocation and reduced CCN2 expression. Dermal fibroblasts were treated with DMSO (CTRL) or Lat-A (180 nM) for 24 hours. After extensive washing, fresh culture media was added for 24 hours. (**a**) Dermal fibroblast size is restored by removal of Lat-A. (**b**) Restoring dermal fibroblast size reversed the impediment of YAP/TAZ nuclear translocation. (**c**) Restoration of dermal fibroblast size reversed CCN2 expression. Cells were immunostained with CCN2 (red) or phalloidin (red), alongside YAP/TAZ (green) and were quantified by ImageJ (National Institutes of Health, Bethesda, MD). Protein levels were expressed in staining intensity after normalization by cell count. Nuclei were stained with DAPI (blue). Data are representative of three independent experiments. Mean ± SEM. $*P < 0.05$. Bar = 50 μm. CTRL, control; Lat-A, Latrunculin-A.

hyaluronic acid) into aged human skin in vivo increases fibroblast spreading and size, thereby restoring CCN2 and type I collagen expression (Quan et al., 2013b). These data suggest that fibroblasts in aged human skin retain the ability to be functionally restored. The capacity to be restored can be mediated by the enhancement of structural and mechanical support in the collagen microenvironment, which increases cell size and spreading. Accordingly, age-related reductions in fibroblast size may be an important mechanism underlying human dermal aging.

We report that in response to changes in cell size, dermal fibroblast expression of CCN2 is largely regulated by YAP/TAZ activity. *CCN2* is identified as a direct YAP/TAZ-target gene, but the exact dynamics of this relationship are not well-known. It is often reported that CCN2 is a simple readout of YAP/TAZ activity (Moroishi et al., 2015; Zhao et al., 2011) rather than a functional effector of YAP/TAZ signaling. We show that decreases in YAP/TAZ expression, in response to reduced cell size, are responsible for the loss of CCN2 expression and subsequent reduced production of type I collagen. The expression and function of YAP/TAZ in the human dermis have not been previously reported. To the best of our knowledge, this report describes a previously unreported downregulation of CCN2 as a result of impeded YAP/TAZ activity, contributing to human dermal aging. We previously reported that impeded YAP/TAZ activity due to reduced fibroblast size is responsible for age-related elevation of hepatocyte GF expression (Xiang et al., 2021). Interestingly, CCN2 partially mediates cell size–dependent upregulation of hepatocyte GF expression through impeded YAP/TAZ nuclear translocation. In aged human skin, hepatocyte GF is elevated in dermal fibroblasts and thus contributes to dermal aging (thin dermis) by the suppression of collagen production. Age-related deterioration of the dermal ECM drives cellular aging by altering fibroblast spreading/mechanical force and consequent functional alterations of YAP/TAZ/CCN2 axis. As such, YAP/TAZ/CCN2 axis may play a critical role in dermal ECM homeostasis.

It is important to note that YAP/TAZ protein expression is lower in aged than in young dermis. However, *YAP/TAZ* mRNA expression is similar between young and aged dermis (Figure 6d), suggesting that post-translational mechanisms may be involved in the downregulation of YAP/TAZ. Additional studies are warranted to elucidate the precise molecular mechanism by which YAP/TAZ is downregulated in aged human skin. Some of the other limitations of our study should also be considered. Notably, we manipulate cells size using Lat-A, which rapidly causes actin depolymerization and consequently cell morphological change. For obvious reasons, in addition to cell morphological change, actin depolymerization affects numerous dynamic cellular processes, including cell migration, cytokinesis, membrane trafficking, and transcriptional regulation, such as MRTF—SRF and YAP/TAZ activity (Gegenfurtner et al., 2018). To confirm the data

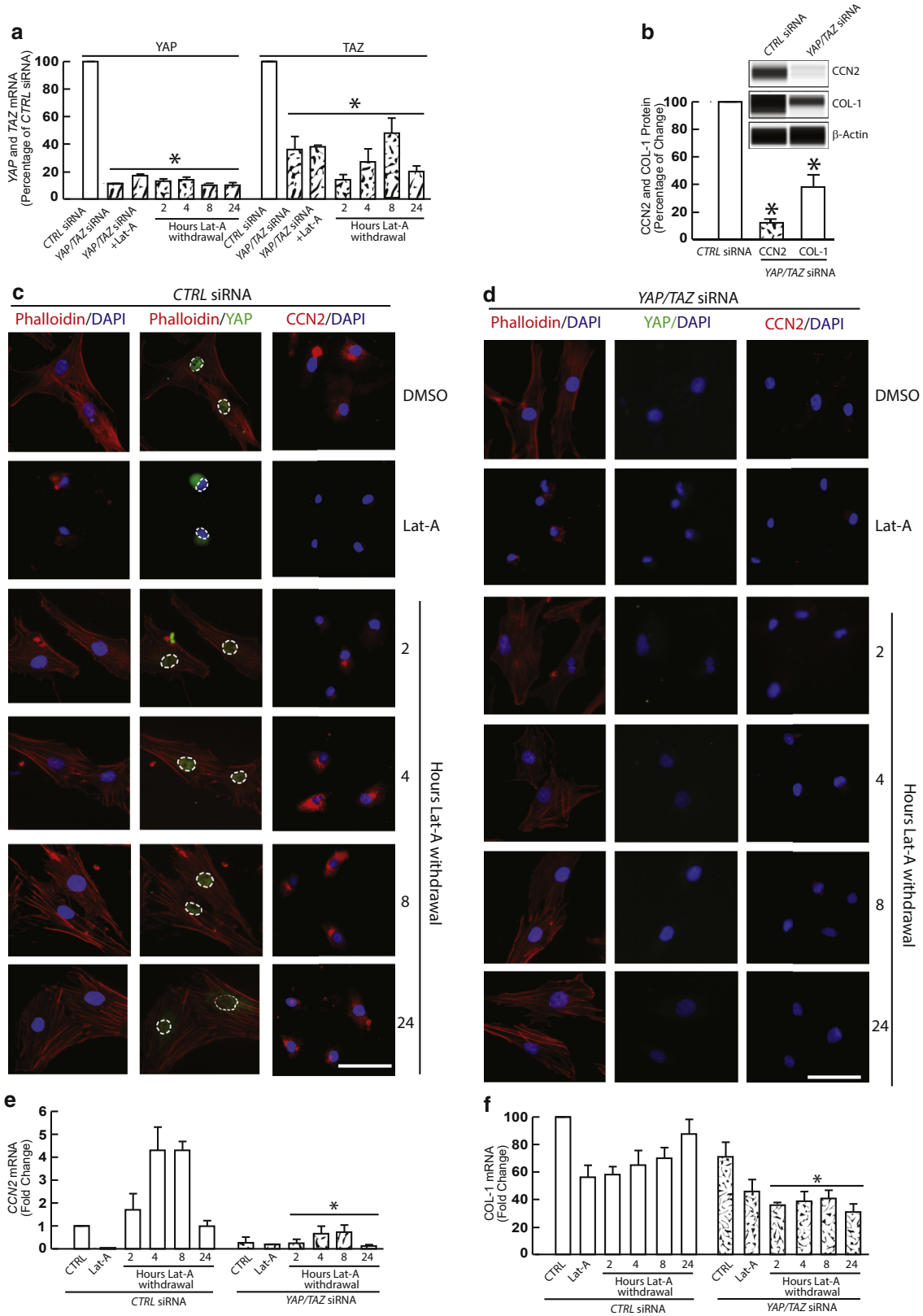

Figure 5. Cell size–dependent reversibility of CCN2 and COL-1 expression is mediated by YAP/TAZ activity. (**a**) Dermal fibroblasts were transfected with control or *YAP/TAZ* siRNA for 32 hours. Cells were then treated with DMSO (CTRL) or Lat-A (180 nM) for 16 hours, extensively washed, and incubated with fresh media for the indicated times. *YAP* and *TAZ* mRNA levels were quantified by real-time RT-PCR and normalized to the housekeeping gene *36B4*, as an internal control for quantification. Data are representative of three independent experiments. Mean ± SEM. *$P < 0.05$. (**b**) Dermal fibroblasts were transfected with control or YAP/TAZ siRNA for 48 hours. CCN2 and CO-1 protein levels were quantified by capillary electrophoresis immunoassay and normalized to β-actin (loading control). The chemiluminescence signal of the specific protein from the capillary tube was obtained directly from the capillary system (Compass software, ProteinSimple, Santa Clara, CA), and the data were displayed by lane in a virtual-blot image, which was simulated using the signal intensity

generated from Lat-A–treated cells, we limited cell size without actin depolymerization. We believe that culturing cells in 3D-broken collagen gel mimics aged fragmented dermal collagen environment. Because there is no established in vitro model that recapitulates the features of aged human skin dermis, we feel justified in our data obtained through four different conditions to manipulate cell size: (i) Lat-A–treated cell, (ii) culturing cells in 3D-broken collagen gel, (iii) culturing cells in integrin-independent plate, and (iv) and culturing the cell in mechanically unconstrained or constrained 3D collagen matrices.

Some recent papers are also noticed, linking CCN2 to a YAP/TAZ feedback loop through paracrine signaling. Shome et al. (2020) recently reported that dermal fibroblasts activation of YAP stimulates CCN2 secretion, which in turn through paracrine signaling activates keratinocytes, accelerates migration, and promotes wound healing. Conversely, cystic epithelial cells stimulate myofibroblast activation in the pericystic microenvironment, leading to fibrosis through the activation of YAP and stimulation of CCN2 expression (Dwivedi et al., 2020). It also should be noted that YAP/TAZ–CCN2 axis may function as an important mediator in fibrosis through myofibroblast activation and ECM production. YAP nuclear localization/activation is exquisitely sensitive to cell size and mechanical tension (Dupont et al., 2011), and constitutive nuclear localization of YAP is a feature of lesional systemic sclerosis dermal fibroblasts (Toyama et al., 2018; Zanconato et al., 2016). In supporting this notion, a recent work shows that blocking YAP activity using a selective YAP inhibitor verteporfin selectively blocks profibrotic gene expression in both normal fibroblasts and fibroblasts from fibrotic lesions of patients with diffuse cutaneous systemic sclerosis (Shi-Wen et al., 2021). YAP inhibitor verteporfin not only selectively reduced the expression of fibrogenic genes but also blocked the ability of TGF-β to induce actin stress fibers in dermal fibroblasts. Consistently, recent work has suggested that YAP inhibitor verteporfin inhibits dermal fibroblast activation and ECM production and thus prevents fibrotic scarring (Mascharak et al., 2021). YAP may function as an important mediator of myofibroblast activation and ECM production, suggesting that pharmacologic approaches targeting the YAP/TAZ–CCN2 molecular axis may have implications for treatment of fibrosis and antiscarring therapies.

In summary, we show that CCN2 is significantly downregulated in aged human dermal fibroblasts in vivo. Mechanistically, reduced fibroblast size, a prominent feature of aged human skin, induces the downregulation of CCN2. This cell size–dependent downregulation of CCN2 is mediated by impeded YAP/TAZ nuclear translocation. These data reveal a mechanism by which age-related reduction of fibroblast size may be an important mechanism underlying human dermal aging by downregulation of CCN2 in a YAP/TAZ-dependent manner.

MATERIALS AND METHODS

Human skin tissues and LCM-coupled quantitative real-time RT-PCR

All procedures involving human volunteers were approved by the University of Michigan (Ann Harbor, MI) Institutional Review Board, and all volunteers provided written informed consent. Skin punch biopsies (4 mm) were obtained from young (mean age of 27 ± 1 years, n = 6) and aged (mean age of 83 ± 1.4 years, n = 6) healthy, sun-protected buttock skin. LCM was performed as previously described (Qin et al., 2017). Briefly, human skin punch biopsies were embedded in an optimal cutting temperature compound before cryostat sectioning. Cryostat sections cut at 15 μm were then mounted on LCM Membrane Slides (Leica Microsystems, Wetzlar, Germany). LCM slides were stained using HistoGene LCM Slide Preparation Kits (Arcturus Therapeutics, San Diego, CA). Dermal fibroblasts (approximately 200 cells) were captured from each sample using LCM (Leica ASLMD System, Leica Microsystems). The identity of the dermal fibroblasts was monitored by identifying the presence of enriched type I procollagen mRNA (dermal fibroblast marker) and the absence of keratin 14 mRNA (epidermal keratinocyte marker) (data not shown). Total RNA was prepared from LCM-captured dermal fibroblasts using a commercial kit (RNeasy Micro kit, Qiagen, Chatsworth, CA). TaqMan PreAmp Master Mix kit (Applied Biosystems, Carlsbad, CA) was used to preamplify cDNA for quantitative real-time PCR. The quality and quantity of amplified cDNA were determined by an Agilent 2100 bioanalyzer (Agilent Technologies, Santa Clara, CA). Quantification of the transcript levels of several different genes in samples of total RNA and amplified cDNA yielded essentially identical results (data not shown). All PCR primers were purchased from RealTimePrimers.com (Elkins Park, PA). Target gene mRNA was

(chemiluminescence) of the specific protein. The chemiluminescence signals of the CCN2 and COL-1 were normalized to β-actin (loading control), and the data were expressed as a percent of control (bar chart). Data are representative of three independent experiments. Mean ± SEM. $*P < 0.05$. (**c, d**) Dermal fibroblasts were transfected with (**c**) CTRL or (**d**) YAP/TAZ siRNA for 32 hours and treated as in Figure 5a. Cells were immunostained with YAP/TAZ (green), phalloidin staining (red), as well as CCN2 (red) separately. Blue fluorescence with dot lines delineates the nuclei (DAPI). Images are representative of three independent experiments. Bar = 100 μm. (**e–g**) Dermal fibroblasts were treated as in Figure 5a. Total RNA was prepared and (**e**) *CCN2* and (**f**) type I procollagen mRNA levels were quantified by real-time RT-PCR and normalized to the housekeeping gene *36B4*, as an internal control for quantification. Data are representative of three independent experiments. Mean ± SEM. $*P < 0.05$. (**g**) COL-1 protein expression was determined by capillary electrophoresis immunoassay and normalized to β-actin (loading control). The chemiluminescence signal of the specific protein from the capillary tube was obtained directly from the capillary system (Compass software, ProteinSimple, Santa Clara, CA), and the data were displayed by lane in a virtual-blot image, which was simulated using the signal intensity (chemiluminescence) of the specific protein. The chemiluminescence signals of COL-1 were normalized to β-actin (loading control), and the data were expressed as a percent of control (bar chart). Data are representative of three independent experiments. Mean ± SEM. $*P < 0.05$ versus CTRL/CTRL siRNA, $**P < 0.05$ versus Lat-A/CTRL siRNA, $***P < 0.05$ versus Lat-A withdrawal/CTRL siRNA. (**h**) Dermal fibroblasts were transfected with control or YAP/TAZ siRNA for 48 hours and then cultured in unconstrained (left) or constrained (middle and right) three-dimensional collagen matrices (see Materials and Methods for details). Cells were immunostained with CCN2, COL-1, and YAP/TAZ. CCN2 protein levels were quantified by ImageJ (National Institutes of Health, Bethesda, MD) and expressed in staining intensity after normalization by cell count. Blue fluorescence (DAPI) shows the nuclei. Data are representative of four independent experiments. Bar = 100 μm. Bar for collagen gel (top panels) = 1 cm. Mean ± SEM. N = 4. $*P < 0.05$ versus unconstrained CTRL siRNA and $**P < 0.05$ versus constrained CTRL siRNA. COL-1, type 1 collagen; CTRL, control; Lat-A, latrunculin-A; siRNA, small interfering RNA.

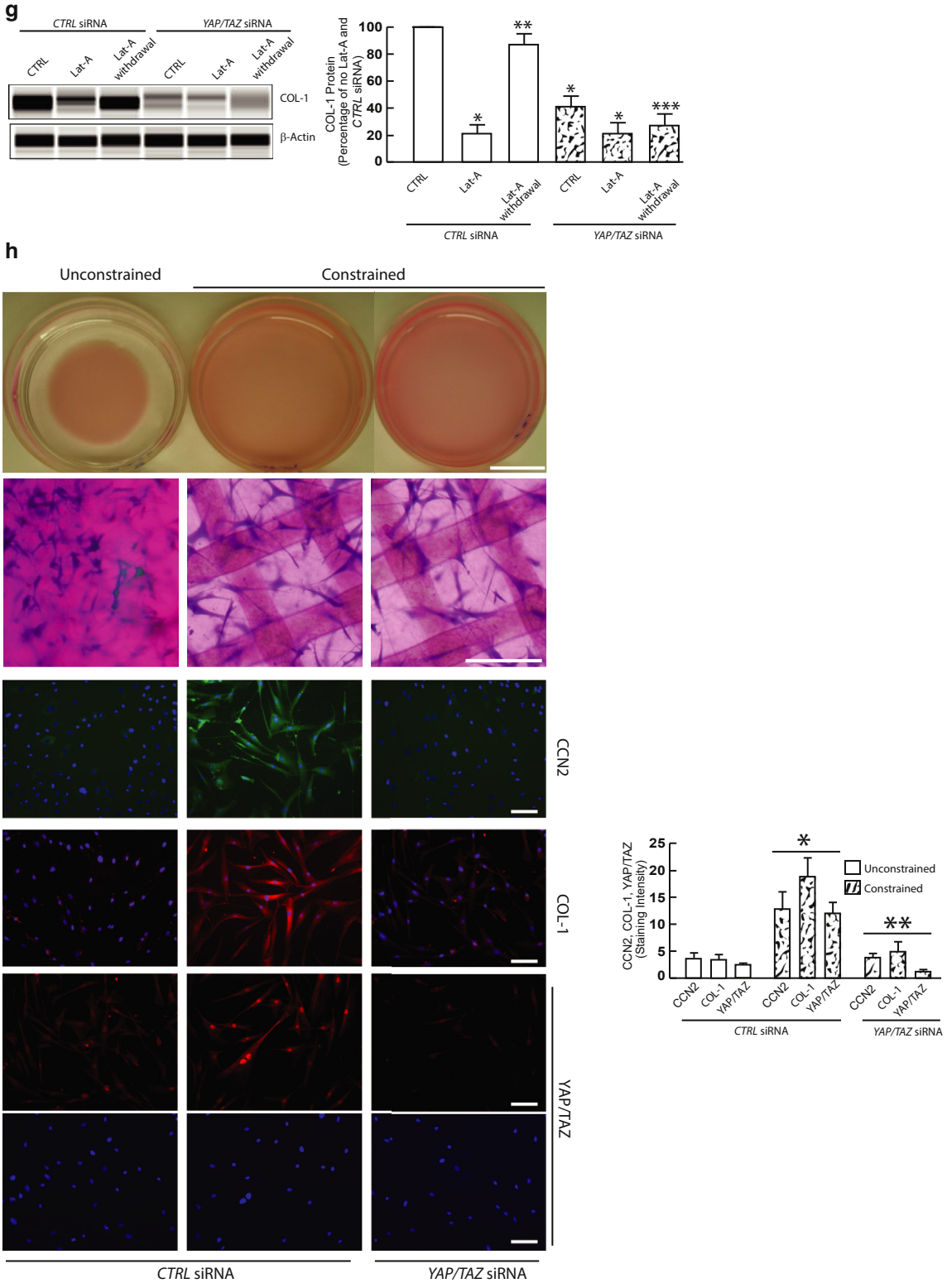

Figure 5. Continued.

normalized to the housekeeping gene *36B4* as an internal control.

Cell culture

Young (mean age of 27 ± 1 years, n = 6) and aged (mean age of 83 ± 1.4 years, n = 6) human dermal fibroblasts were prepared from sun-protected buttock skin as previously described (Fisher et al., 1991). Primary dermal fibroblasts were isolated from skin digested with bacterial collagenase (Worthington Biochemical, Lakewood, NJ) and plated on a six-well plate in DMEM media (Life Technology, Carlsbad, CA) without passage. Early passage (<9 passages) primary adult human dermal fibroblasts were cultured in DMEM with 10%

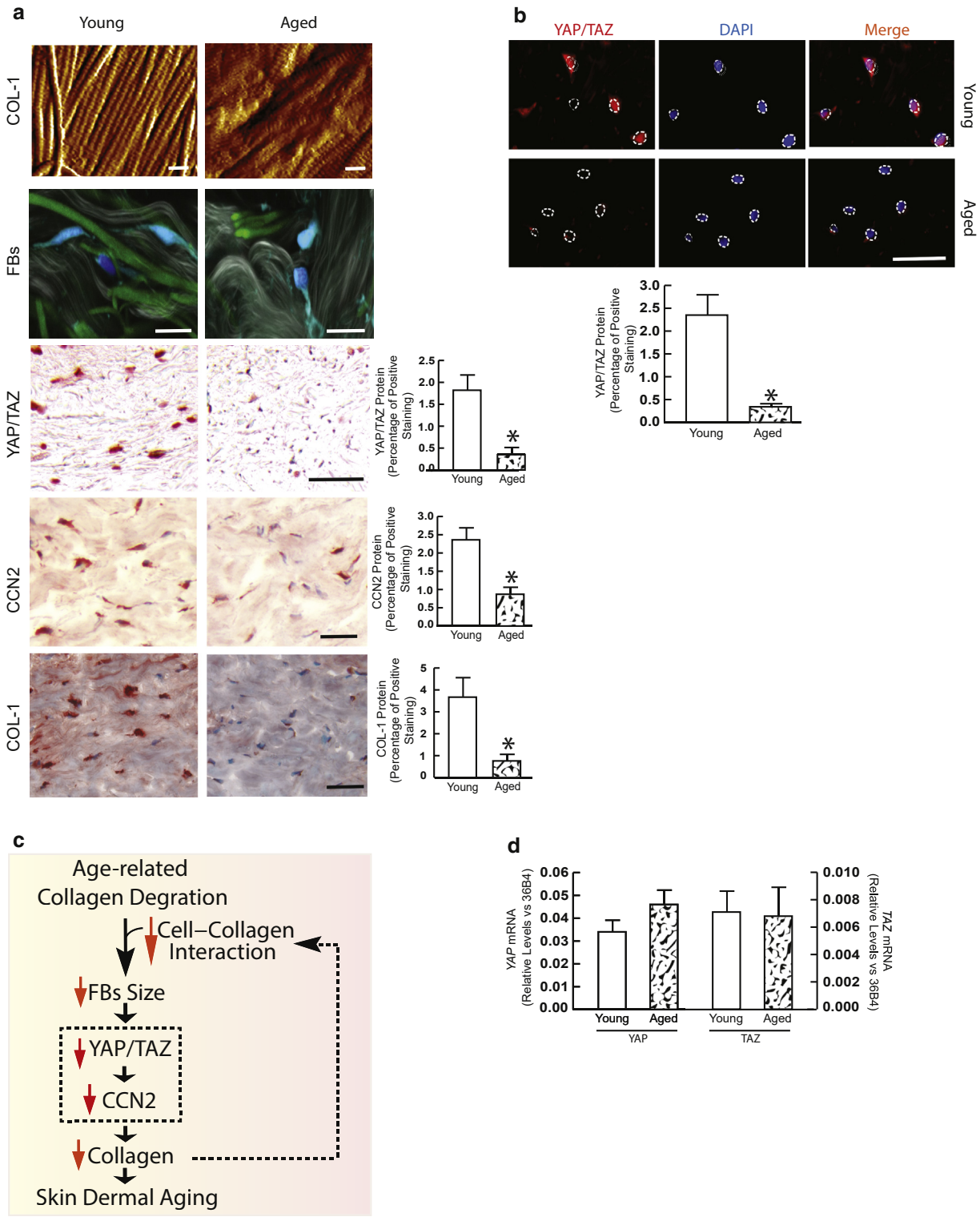

Figure 6. Downregulation of YAP/TAZ, CCN2, and COL-1 in aged human skin in vivo. (**a**) Human skin biopsies were obtained from young (left, n = 6) and aged (right, n = 6) sun-protected buttock skin. Nanoscale images of collagen fibrils were imaged by AFM (top). Collagen fiber (white), elastin fiber (green), and fibroblast morphology were imaged by multiphoton laser scanning fluorescence microscopy (second from top). YAP/TAZ (middle), CCN2 (second to last), and type I procollagen (bottom) protein expressions were assessed by immunohistochemistry. Images are representative of six subjects from each age group. YAP/TAZ, CCN2, and COL-1 protein levels were quantified by ImageJ (National Institutes of Health, Bethesda, MD) and expressed in the percent of positive staining. Data represent six young and six aged subjects. Mean ± SEM. *$P < 0.05$. Bars for AFM = 200 nm, for multiphoton laser scanning fluorescence microscopy = 25 μm, for YAP/TAZ = 50 μm, for CCN2 = 50 μm, and for COL-1 = 50 μm. (**b**) YAP/TAZ immunofluorescence staining in young and aged human skin. Blue fluorescence with dot lines delineates the nuclei (DAPI). YAP/TAZ protein levels were quantified by ImageJ and expressed in the percent of positive staining. Note the less YAP/TAZ nuclear staining in the aged dermis. Data represent six young and six aged subjects. Mean ± SEM. *$P < 0.05$. Bar = 25 μm. (**c**) Age-related reduced fibroblast size concomitantly downregulates YAP/TAZ activity and CCN2 expression in aged human skin. Age-related collagen fragmentation is

fetal calf serum (Life Technology) at 37 °C and 5% carbon dioxide. The approximate population doubling time was 2 days. The 3D collagen gels were prepared on the basis of a previous publication, with minor modifications (Qin et al., 2014a). Briefly, neutralized rat tail type I collagen (2 mg/ml, BD Biosciences, Palo Alto, CA) was suspended in a medium cocktail (DMEM, sodium bicarbonate [44 mM], L-glutamine [4 mM], and folic acid [9 mM], neutralized with 1 N sodium hydroxide to pH 7.2). Cells (0.5×10^6) were suspended in 2 ml of collagen and medium cocktail solution and plated in a 35-mm bacterial culture dish. The collagen gels were then incubated with 2 ml of media (DMEM, 10% fetal bovine serum) at 37°C and 5% carbon dioxide. Partially degraded collagen lattices were prepared by treatment with purified human matrix metalloproteinase 1 (50 ng per well, Calbiochem, San Diego, CA) for 16 hours at 37 °C (Fisher et al., 2009). In some experiments, the cells were cultured in mechanically constrained or unconstrained 3D collagen matrices. The mechanical constraint was achieved by incorporating a nylon mesh disk within the collagen gel (Fisher et al., 2016). For Lat-A (Sigma-Aldrich, St. Louis, MO) treatment, cells were treated with Lat-A at a concentration of 180 nM for 24 hours.

Human primary skin fibroblasts were transiently transfected with YAP/TAZ-mutant plasmids (Chan et al., 2011) (kindly provided by Chan SW, Institute of Molecular and Cell Biology, Agency for Science, Technology and Research, Singapore, Singapore) and *YAP/TAZ* siRNAs by electroporation (Amaxa Biosystems, Koeln, Germany). YAP/TAZ-mutant plasmids were generated by introducing the amino acid mutations (YAP-S127AS and TAZ-S89A) in YAP- and TAZ-coding regions, which prevent YAP and TAZ ubiquitination and proteasomal degradation and promote constitutive YAP/TAZ nuclear translocation (Chan et al., 2011). Transient transfection of Emerald GFP (The Vivid Colors, Thermo Fisher Scientific, Waltham, MA) indicated that the transfection efficiency can be up to 80% in human primary skin fibroblasts by electroporation. siRNAs for the first set of *YAP* (GACAUCUUCUGGUCAGAGA) and *TAZ* (AGGUACUUCCUCAAUCACA) and for the second set of *YAP* (CUGGUCAGAGAUACUUCUU) and *TAZ* (ACGUUGACUUAGGAACUUU) were purchased from Sigma-Aldrich. Control siRNA (AATTGTCCGAACGTGTCACGT) were purchased from Qiagen.

Human dermis western blotting

To assess CCN2 protein expression in the dermis, the epidermis was removed using a cryostat to cut to a depth of 1 mm and was confirmed by H&E staining (Figure 1d). For western blot analysis, dermal tissues were ground into a fine powder in liquid nitrogen and homogenized by Polytron in a whole-cell extraction buffer. Approximately 100 μg of protein was resolved by 12% SDS-PAGE, transferred to a polyvinylidene difluoride membrane, and blocked with 0.1% Tween 20 in PBS containing 5% milk for 1 hour at room temperature. The primary antibodies against CCN2 (catalog number sc-101586, 1:100, Santa Cruz Biotechnology, Santa Cruz, CA), YAP/TAZ (catalog number 93622, 1:1,000, Cell Signaling Technology, Danvers, MA), type I procollagen (catalog number 1310-01, 1:500, SouthernBiotech, Birmingham, AL), and β-actin (catalog number A2228, 1:1,000, Sigma-Aldrich) were incubated with a polyvinylidene difluoride membrane for 1 hour at room temperature. Blots were washed three times with 0.1% Tween 20 in PBS solution and incubated with the appropriate secondary antibody (catalog numbers 7074 and 7056, Cell Signaling Technology) for 1 hour at room temperature. After washing three times with 0.1% Tween 20 in PBS, the blots were developed with ECF (Vistra ECF Western Blotting System, Amersham Pharmacia Biotech, Piscataway, NJ) following the manufacturer's instructions (Molecular Dynamics, Sunnyvale, CA). The intensities of each band were normalized to β-actin (Sigma-Aldrich) as an internal control.

Immunostaining and phalloidin staining

For immunostaining, optimal cutting temperature–embedded skin sections or cells were fixed in 2% paraformaldehyde for 2 hours at room temperature. The sections were incubated with 0.5% Nonidet P-40 and then blocked with 2% BSA. The slides were washed with PBS several times and incubated with primary antibodies: YAP/TAZ (catalog number 93622, 1:50, Cell Signaling Technology), CCN2 (catalog number AF660, dilution 15 μg/ml, R&D Systems, Minneapolis, MN), and type I collagen (catalog number ab6308, 4 μg/ml, Abcam, Waltham, MA) for 1 hour at room temperature. Cells were washed and then incubated with a secondary antibody (catalog numbers 7074 and 7056, Cell Signaling Technology; catalog number sc-2359, Santa Cruz Biotechnology) for 30 minutes at room temperature. Images were obtained using a Zeiss fluorescence microscope. Cell morphology was assessed by the incubation of cultures with phalloidin. Briefly, cells were washed with PBS and fixed in 2% paraformaldehyde for 30 minutes, followed by phalloidin staining (Sigma-Aldrich) for 1 hour.

ProteinSimple capillary electrophoresis immunoassay

The ProteinSimple (Santa Clara, CA) capillary electrophoresis immunoassay was performed according to the ProteinSimple user manual. Briefly, whole-cell and nuclear extract samples (800 ng/lane) were mixed with a master mix (provided by ProteinSimple kit) to a final concentration of ×1 sample buffer, ×1 fluorescent molecular weight markers, and 40 mM dithiothreitol and then heated at 95 °C for 5 minutes. Cytoplasmic and nuclear protein fractions were prepared using nuclear and cytoplasmic extraction reagents (NE-PER, catalog number 78833, Thermo Fisher Scientific). The samples, blocking reagent, primary antibodies (CCN2, catalog number sc-101586, 1:100, Santa Cruz Biotechnology; YAP/TAZ, catalog number 93622, 1:1,000, Cell Signaling Technology; type I procollagen, catalog number 1310-01, 1:500, SouthernBiotech; β-actin, catalog number A2228, 1:1,000, Sigma-Aldrich), horseradish peroxidase–conjugated secondary antibodies (provided from ProteinSimple kit), chemiluminescent substrate, and separation and stacking matrices were also dispensed to designated well plates. The electrophoresis and immunodetection steps were performed in the capillary system (ProteinSimple Wes, ProteinSimple) and were fully automated using default instrument settings. The chemiluminescence signal of the specific protein from the capillary tube was obtained directly from the capillary system (Compass software, ProteinSimple), and the data

a prominent feature of aged human skin, which impairs cell–collagen interaction and alters fibroblast shape and size. Reduced fibroblast size leads to numerous alterations, including impediments of YAP/TAZ activity. Impaired YAP/TAZ activity downregulates CCN2 expression, which in turn contributes to loss of collagen production, a prominent feature of human dermal aging (see Discussion for details). (**d**) *YAP* and *TAZ* mRNA expression in young and aged human skin in vivo. Total RNA was prepared from young and aged sun-protected buttock skin. *YAP* and *TAZ* mRNA levels were quantified by real-time RT-PCR and normalized to the housekeeping gene *36B4*, as an internal control for quantification (lower left). Data are expressed as mean ± SEM. N = 4. AFM, atomic force microscopy; COL-1, type 1 collagen; FB, fibroblast.

were displayed by lane in a virtual-blot image, which was simulated using the signal intensity (chemiluminescence) of the specific protein. For the quantification, Compass software automatically displays the quantitative results such as molecular weight and signal intensity (chemiluminescence) for each immunodetected protein. The chemiluminescence signal of the specific protein was normalized to β-actin (loading control), and the data were expressed as a percent of control.

Atomic force microscopy and second-harmonic generation microscopy

Human skin biopsies were embedded in an optimal cutting temperature compound. To cut skin sections, the tissue block was trimmed, and 15-μm thick skin cryosections were mounted on glass coverslips (1.2-mm diameter, Fisher Scientific, Pittsburgh, PA) and allowed to air dry for at least 24 hours before atomic force microscopy (AFM) analysis. AFM scan positions of the collagen lattices were determined by a light optical image. Images were obtained by AFM in ScanAsyst mode (Dimension Icon, Bruker-AXS, Santa Barbara, CA) in the air using a silicon-etched cantilever (NSC15/AIBS, MikroMasch, San Jose, CA) with a full tip cone angle of $\sim 40^{o}$ and a tip radius curvature of ∼10 nm. AFM images were acquired at a scan rate of 0.977 Hz and 512 × 512 pixel resolution. AFM imaging was conducted at the Electron Microbeam Analysis Laboratory, University of Michigan College of Engineering and analyzed using Nanoscope Analysis software (Nanoscope Analysis, version 120R1sr3, Bruker-AXS, Santa Barbara, CA). Second-harmonic generation images were obtained using a Zeiss fluorescence microscope. Second-harmonic generation microscopy was performed using a Leica SP8 Confocal Microscope at the University of Michigan Microscopy and Image Analysis Laboratory.

Charts and statistics

Charts were generated with Adobe Illustrator (Adobe, San Jose, CA). Bar graphs represent means ± SEM. Statistical analyses were performed using one-way ANOVA with Bonferroni posthoc multiple comparisons. All *P*-values are considered significant when <0.05 (depicted by asterisks on figures).

Data availability statement

No datasets were generated or analyzed during this study.

ORCIDs

Zhaoping Qin: http://orcid.org/0000-0003-2439-5417
Chunfang Guo: http://orcid.org/0000-0002-7574-4069
Tianyuan He: http://orcid.org/0000-0003-4466-6587
Taihao Quan: http://orcid.org/0000-0002-0954-5109

AUTHOR CONTRIBUTIONS

Conceptualization: TQ; Data Curation: ZQ, TH, CG; Formal Analysis: ZQ, TH, TQ; Investigation: ZQ, TH, CG; Methodology: ZQ, TH, CG, TQ; Supervision: TG; Validation: ZQ, TH, CG, TQ; Original Draft Preparation: TQ; Review and Editing: ZQ, TH, CG, TQ. TQ supervised the study. TQ and ZQ analyzed and interpreted the data. TQ wrote the manuscript and all authors commented on the manuscript.

ACKNOWLEDGMENTS

The authors thank John J. Voorhees and Gary J. Fisher for their critical review and suggestions to the manuscript. The authors thank Kenneth Calderone for technical assistance and Joel Maust for providing writing/editorial support. This work was supported by the National Institute of Health (RO1ES014697 and ES014697-03S1 to TQ).

CONFLICT OF INTEREST

The authors state no conflict of interest.

REFERENCES

Ashcroft GS, Horan MA, Ferguson MW. The effects of ageing on cutaneous wound healing in mammals. J Anat 1995;187:1–26.

Ashcroft GS, Mills SJ, Ashworth JJ. Ageing and wound healing. Biogerontology 2002;3:337–45.

Bissell MJ, Hines WC. Why don't we get more cancer? A proposed role of the microenvironment in restraining cancer progression. Nat Med 2011;17:320–9.

Bissell MJ, Kenny PA, Radisky DC. Microenvironmental regulators of tissue structure and function also regulate tumor induction and progression: the role of extracellular matrix and its degrading enzymes. Cold Spring Harb Symp Quant Biol 2005;70:343–56.

Chan SW, Lim CJ, Chong YF, Pobbati AV, Huang C, Hong W. Hippo pathway-independent restriction of TAZ and YAP by angiomotin. J Biol Chem 2011;286:7018–26.

Duncan MR, Frazier KS, Abramson S, Williams S, Klapper H, Huang X, et al. Connective tissue growth factor mediates transforming growth factor β-induced collagen synthesis: down-regulation by cAMP. FASEB J 1999;13:1774–86.

Dupont S, Morsut L, Aragona M, Enzo E, Giulitti S, Cordenonsi M, et al. Role of YAP/TAZ in mechanotransduction. Nature 2011;474:179–83.

Dwivedi N, Tao S, Jamadar A, Sinha S, Howard C, Wallace DP, et al. Epithelial vasopressin type-2 receptors regulate myofibroblasts by a YAP-CCN2-Dependent mechanism in polycystic kidney disease. J Am Soc Nephrol 2020;31:1697–710.

Eaglstein WH. Wound healing and aging. Clin Geriatr Med 1989;5:183–8.

Fisher GJ, Esmann J, Griffiths CE, Talwar HS, Duell EA, Hammerberg C, et al. Cellular, immunologic and biochemical characterization of topical retinoic acid-treated human skin [published correction appears in J Invest Dermatol 1991;96:814]. J Invest Dermatol 1991;96:699–707.

Fisher GJ, Quan T, Purohit T, Shao Y, Cho MK, He T, et al. Collagen fragmentation promotes oxidative stress and elevates matrix metalloproteinase-1 in fibroblasts in aged human skin. Am J Pathol 2009;174:101–14.

Fisher GJ, Shao Y, He T, Qin Z, Perry D, Voorhees JJ, et al. Reduction of fibroblast size/mechanical force down-regulates TGF-β type II receptor: implications for human skin aging. Aging Cell 2016;15:67–76.

Fisher GJ, Varani J, Voorhees JJ. Looking older: fibroblast collapse and therapeutic implications. Arch Dermatol 2008;144:666–72.

Gegenfurtner FA, Zisis T, Al Danaf N, Schrimpf W, Kliesmete Z, Ziegenhain C, et al. Transcriptional effects of actin-binding compounds: the cytoplasm sets the tone. Cell Mol Life Sci 2018;75:4539–55.

Geiger B, Spatz JP, Bershadsky AD. Environmental sensing through focal adhesions. Nat Rev Mol Cell Biol 2009;10:21–33.

Gieni RS, Hendzel MJ. Mechanotransduction from the ECM to the genome: are the pieces now in place? J Cell Biochem 2008;104:1964–87.

Ingber DE. Can cancer be reversed by engineering the tumor microenvironment? Semin Cancer Biol 2008;18:356–64.

Ivkovic S, Yoon BS, Popoff SN, Safadi FF, Libuda DE, Stephenson RC, et al. Connective tissue growth factor coordinates chondrogenesis and angiogenesis during skeletal development. Development 2003;130:2779–91.

Jacob MP. Extracellular matrix remodeling and matrix metalloproteinases in the vascular wall during aging and in pathological conditions. Biomed Pharmacother 2003;57:195–202.

Kapoor M, Liu S, Huh K, Parapuram S, Kennedy L, Leask A. Connective tissue growth factor promoter activity in normal and wounded skin. Fibrogenesis Tissue Repair 2008;1:3.

Kubota S, Takigawa M. Cellular and molecular actions of CCN2/CTGF and its role under physiological and pathological conditions [published correction appears in Clin Sci (Lond) 2015;129:674]. Clin Sci (Lond) 2015;128:181–96.

Lavker RM. Structural alterations in exposed and unexposed aged skin. J Invest Dermatol 1979;73:59–66.

Leask A. Conjunction junction, what's the function? CCN proteins as targets in fibrosis and cancers. Am J Physiol Cell Physiol 2020;318:C1046–54.

Leask A, Holmes A, Black CM, Abraham DJ. Connective tissue growth factor gene regulation. Requirements for its induction by transforming growth factor-beta 2 in fibroblasts. J Biol Chem 2003;278:13008–15.

Liu S, Parapuram SK, Leask A. Fibrosis caused by loss of PTEN expression in mouse fibroblasts is crucially dependent on CCN2. Arthritis Rheum 2013;65:2940–4.

Liu S, Taghavi R, Leask A. Connective tissue growth factor is induced in bleomycin-induced skin scleroderma. J Cell Commun Signal 2010;4: 25–30.

Mascharak S, desJardins-Park HE, Davitt MF, Griffin M, Borrelli MR, Moore AL, et al. Preventing Engrailed-1 activation in fibroblasts yields wound regeneration without scarring. Science 2021:372.

Mazia D, Schatten G, Sale W. Adhesion of cells to surfaces coated with polylysine. Applications to electron microscopy. J Cell Biol 1975;66:198–200.

McLennan SV, Abdollahi M, Twigg SM. Connective tissue growth factor, matrix regulation, and diabetic kidney disease. Curr Opin Nephrol Hypertens 2013;22:85–92.

Moroishi T, Hansen CG, Guan KL. The emerging roles of YAP and TAZ in cancer. Nat Rev Cancer 2015;15:73–9.

Moussad EE, Brigstock DR. Connective tissue growth factor: what's in a name? Mol Genet Metab 2000;71:276–92.

Moya IM, Halder G. Hippo-YAP/TAZ signalling in organ regeneration and regenerative medicine. Nat Rev Mol Cell Biol 2019;20:211–26.

Panciera T, Azzolin L, Cordenonsi M, Piccolo S. Mechanobiology of YAP and TAZ in physiology and disease. Nat Rev Mol Cell Biol 2017;18:758–70.

Perbal B. CCN proteins: multifunctional signalling regulators. Lancet 2004;363:62–4.

Pickup MW, Mouw JK, Weaver VM. The extracellular matrix modulates the hallmarks of cancer. EMBO Rep 2014;15:1243–53.

Qin Z, Balimunkwe RM, Quan T. Age-related reduction of dermal fibroblast size upregulates multiple matrix metalloproteinases as observed in aged human skin in vivo. Br J Dermatol 2017;177:1337–48.

Qin Z, Okubo T, Voorhees JJ, Fisher GJ, Quan T. Elevated cysteine-rich protein 61 (CCN1) promotes skin aging via upregulation of IL-1β in chronically sun-exposed human skin. Age (Dordr) 2014a;36:353–64.

Qin Z, Voorhees JJ, Fisher GJ, Quan T. Age-associated reduction of cellular spreading/mechanical force up-regulates matrix metalloproteinase-1 expression and collagen fibril fragmentation via c-Jun/AP-1 in human dermal fibroblasts. Aging Cell 2014b;13:1028–37.

Quan T, Fisher GJ. Role of age-associated alterations of the dermal extracellular matrix microenvironment in human skin aging: a mini-review. Gerontology 2015;61:427–34.

Quan T, Little E, Quan H, Qin Z, Voorhees JJ, Fisher GJ. Elevated matrix metalloproteinases and collagen fragmentation in photodamaged human skin: impact of altered extracellular matrix microenvironment on dermal fibroblast function. J Invest Dermatol 2013a;133:1362–6.

Quan T, Shao Y, He T, Voorhees JJ, Fisher GJ. Reduced expression of connective tissue growth factor (CTGF/CCN2) mediates collagen loss in chronologically aged human skin. J Invest Dermatol 2010;130:415–24.

Quan T, Wang F, Shao Y, Rittié L, Xia W, Orringer JS, et al. Enhancing structural support of the dermal microenvironment activates fibroblasts, endothelial cells, and keratinocytes in aged human skin in vivo. J Invest Dermatol 2013b;133:658–67.

Shi-Wen X, Racanelli M, Ali A, Simon A, Quesnel K, Stratton RJ, et al. Verteporfin inhibits the persistent fibrotic phenotype of lesional scleroderma dermal fibroblasts. J Cell Commun Signal 2021;15:71–80.

Shome D, von Woedtke T, Riedel K, Masur K. The HIPPO transducer YAP and its targets CTGF and Cyr61 drive a paracrine signalling in cold atmospheric plasma-mediated wound healing. Oxid Med Cell Longev 2020;2020: 4910280.

Thomas DR. Age-related changes in wound healing. Drugs Aging 2001;18: 607–20.

Toyama T, Looney AP, Baker BM, Stawski L, Haines P, Simms R, et al. Therapeutic targeting of TAZ and YAP by dimethyl fumarate in systemic sclerosis fibrosis. J Invest Dermatol 2018;138:78–88.

Twigg SM. Regulation and bioactivity of the CCN family of genes and proteins in obesity and diabetes. J Cell Commun Signal 2018;12:359–68.

Uitto J. Connective tissue biochemistry of the aging dermis. Age-related alterations in collagen and elastin. Dermatol Clin 1986;4:433–46.

Uitto J, Bernstein EF. Molecular mechanisms of cutaneous aging: connective tissue alterations in the dermis. J Investig Dermatol Symp Proc 1998;3:41–4.

Urtasun R, Latasa MU, Demartis MI, Balzani S, Goñi S, Garcia-Irigoyen O, et al. Connective tissue growth factor autocriny in human hepatocellular carcinoma: oncogenic role and regulation by epidermal growth factor receptor/yes-associated protein-mediated activation. Hepatology 2011;54: 2149–58.

Varani J, Schuger L, Dame MK, Leonard C, Fligiel SE, Kang S, et al. Reduced fibroblast interaction with intact collagen as a mechanism for depressed collagen synthesis in photodamaged skin. J Invest Dermatol 2004;122:1471–9.

Xiang Y, Qin Z, Yang Y, Fisher GJ, Quan T. Age-related elevation of HGF is driven by the reduction of fibroblast size in a YAP/TAZ/CCN2 axis-dependent manner. J Dermatol Sci 2021;102:36–46.

Zanconato F, Battilana G, Cordenonsi M, Piccolo S. YAP/TAZ as therapeutic targets in cancer. Curr Opin Pharmacol 2016;29:26–33.

Zhao B, Li L, Guan KL. Hippo signaling at a glance. J Cell Sci 2010;123: 4001–6.

Zhao B, Tumaneng K, Guan KL. The Hippo pathway in organ size control, tissue regeneration and stem cell self-renewal. Nat Cell Biol 2011;13: 877–83.